INTERNATIONAL JOURNAL OF DIGITAL INFORMATION AND WIRELESS COMMUNICATIONS (IJDIWC) 1(1): 1-13
THE SOCIETY OF DIGITAL INFORMATION AND WIRELESS COMMUNICATIONS, 2011 (ISSN 2225-658X)

Automatic Registration of Cerebral Vascular Structures

Marwa HERMASSI, Hejer JELASSI and Kamel HAMROUNI
BP 37, Le Belvédère 1002 Tunis, Tunisia
m.hermassi@gmail.com, kamel.hamrouni@enit.rnu.tn, hejer_enit@yahoo.fr

ABSTRACT

In this paper we present a registration method for cerebral vascular structures in the 2D MRA images. The method is based on bifurcation structures. The usual registration methods, based on point matching, largely depend on the branching angels of each bifurcation point. This may cause multiple feature correspondence due to similar branching angels. Hence, bifurcation structures offer better registration. Each bifurcation structure is composed of a master bifurcation point and its three connected neighbors. The characteristic vector of each bifurcation structure consists of the normalized branching angle and length, and it is invariant against translation, rotation, scaling, and even modest distortion. The validation of the registration accuracy is particularly important. Virtual and physical images may provide the gold standard for validation. Also, image databases may in the future provide a source for the objective comparison of different vascular registration methods.

KEYWORDS

Bifurcation structures, bifurcation points, branching angles, feature extraction, image registration, vascular structures.

1 INTRODUCTION

Image registration is the process of establishing pixel-to-pixel correspondence between two images of the same scene. It's quite difficult to have an overview on the registration methods due to the important number of publications concerning this subject such as [1] and [2]. Some authors presented excellent overview of medical images registration methods [3], [4] and [5]. From these works, we can say that image registration is based on four elements: features, similarity criterion, transformation and finally, optimization method. Many registration approaches are described in the literature. They can be classified in three categories: Geometric approaches or feature-feature registration methods, volumetric approaches also known as image-image approaches and finally mixed methods. The first methods consist on automatically or manually extracting features from image. Features can be significant regions, lines or points. They should be distinct, spread all over the image and efficiently detectable in both images. They are also expected to be stable in time to stay at fixed positions during the whole experiment [2]. The second approaches optimize a similarity measure that directly compares voxel intensities between two images. These registration methods are favored for registering tissue images [6]. The mixed methods are combinations between the two methods cited before. [7] developed an approach based on block matching using volumetric features combined to a geometric algorithm: the Iterative Closest Point algorithm (ICP). The ICP algorithm uses the distance between surfaces and lines in images. Distance is

a geometric similarity criterion, the same as the Hausdorff distance or the distance maps such as used in [8] and [9]. The Euclidian distance is used to match points features. On the other hand volumetric criterion are based on points intensity such as the Lowest Square (LS) criterion used in monomodal registration, correlation coefficient, correlation factor, Woods criterion [10] and the Mutual Information [11]. The third element, the transformation, can be linear such as affine, rigid and projective transformations. It can be non linear such as functions base, Radial Basis Functions (RBF) and the Free Form Deformations (FFD). The last step in the registration process is the optimization of the similarity criterion. It consists on maximizing or minimizing the criterion. We can cite the Weighted Least Square [12], the one-plus-one revolutionary optimizer developed by Styner and al. [13] and used by Chillet and al. in [8]. An overview of the optimization methods is presented on [14]. The structure of the cerebral vascular network, shown in figure 1, presents anatomical invariants which motivates for using robust features such as bifurcation points as they are a stable indicator for blood flow.

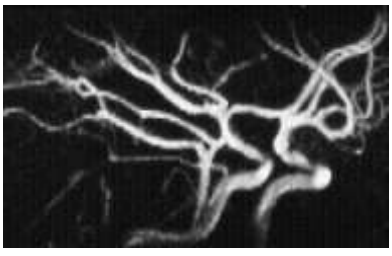

Fig. 1. Vascular cerebral vessels.

Points matching techniques are based on corresponding points on both images. These approaches are composed of two steps: feature matching and transformation estimation. The matching process establishes the correspondence between two features groups. Once the matched pairs are efficient, transformation parameters can be identified easily and precisely. The branching angles of each bifurcation point are used to produce a probability for every pair of points. As these angles have a coarse precision which leads to similar bifurcation points, the matching won't be unique and reliable to guide registration. In this view Chen et al. [15] proposed a new structural characteristic for the feature-based retinal images registration.

The proposed method consists on a structure matching technique. This structure, the bifurcation structure, is composed of a master bifurcation point and its three connected neighbors. The characteristic vector of each bifurcation structure is composed the normalized branching angles and lengths. The idea is to set a transformation obtained from the feature matching process and to perform registration then. If doesn't work, another solution has to be tested to minimize the error. We propose to use this technique to vascular structures in 2D Magnetic Resonance angiographic images.

2 PRETREATMENT STEPS:

2.1 Segmentation:

For the segmentation of the vascular network, we use its connectivity characteristic. [16] proposes a technique based on the mathematical morphology which provides a robust transformation, the morphological construction. It requires two images: a mask image and a marker image and operates by iterating until idem potency a geodesic dilatation

of the marker image with respect to the mask image. Applying a morphological algorithm, named "Toggle mapping", on the original image followed by a transformation "top hat" which extract clear details of the image provides the mask image. This transformation is defined by:

$$f_2 = TM(f_1) = \begin{cases} \phi^{\lambda B}(f_1) \;;\; if \quad (\phi^{\lambda B}(f_1) - f_1) \le (f_1 - \gamma^{sB}(f_1)) \\ \gamma^{sB}(f_1) \qquad else \end{cases} \tag{1}$$

Which f_1 and f_2 are respectively the original image and the image improved, ϕ and γ are the morphological closing and opening and B is the structuring element.

The size of the structuring element is chosen in a way to improve first the vascular vessels borders in the original image, and then to extract all the details which belong to the vascular network. First the clear details of the resulting image of the "toggle mapping" are extracted by the process of "top hat by opening". The resulting image is considered as the image mask. This transformation is defined by:

$$f_3 = f_2 - \gamma^B(f_2) \tag{2}$$

Second the extracted details may contain other parasite or pathological objects which are not connected to the vascular network. To eliminate these objects, we apply the suppremum opening with linear and oriented structuring elements. The resulting image will be considered as the marker image. The equation of the suppremum opening is given by:

$$f_4 = S_{\sup}(f_3) = \max_{L_\theta \in L}(\gamma_{L_\theta}(f_3)) \tag{3}$$

Where $L = \{L_\theta; \theta = 0° \ldots\ldots\ldots\ldots 180°\}$, are the structuring elements.

The morphological construction is finally applied with the obtained mask and marker images according to the equation:

$$f_5 = R_f^{(i)}(f_4) = \delta_{f_3}^i(f_4) \quad with \quad \delta_{f_3}^i(f_4) = \delta_{f_3}^{i+1}(f_4) \tag{4}$$

The result of image segmentation is shown on figure 2.

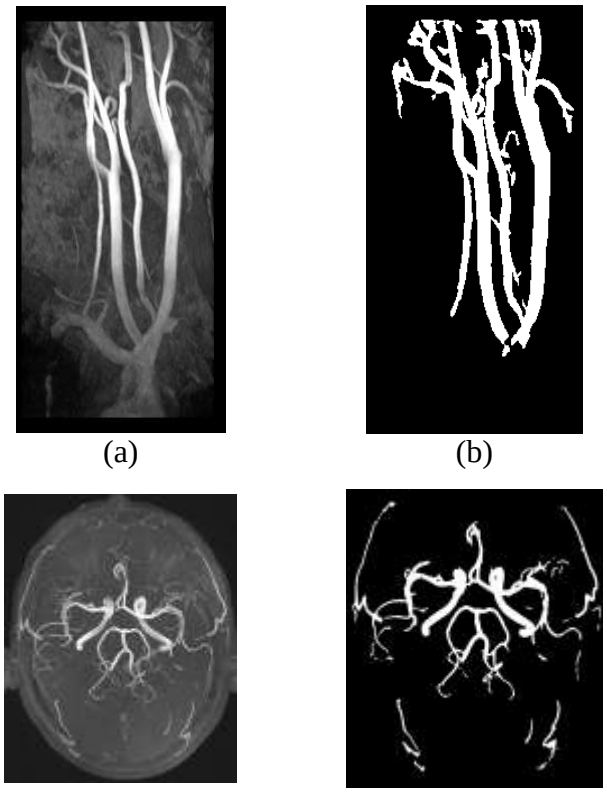

(a) (b) (c) (d)

Fig. 2. Segmentation result. (a) and (c) Original image. (b) and (d)Segmented image.

2.2 Skeletonization:

The skeletonization step is crucial for the registration. Indeed, without this step it becomes difficult

to detect bifurcation points. It consists on reducing a form in a set of lines. Many skeletonization approaches exist such as topological thinning, distance maps extraction, analytical calculation and the burning front simulation. An overview of the skeletonization methods is presented in [17]. In this work, we opt for a topological thinning skeletonization. It consists on eroding little by little the objects' border until the image is centered and thin. Let X be an object of the image and B the structuring element. The skeleton is obtained by removing from X the result of erosion of X by B.

$$X \circ B^i = X \setminus ((((X \ominus B^1) \ominus B^2) \ominus B^3) \ominus B^4) \quad (5)$$

The B^i are obtained following a Π/4 rotation of the structuring element. They are four in number shown in figure 3 (a). Figure 3 (b) shows different iterations of skeletonization of a segmented image.

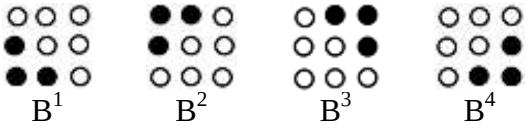

Fig.3 (a). Different structured elements, following a Π/4 rotation.

Initial Image **First iteration**

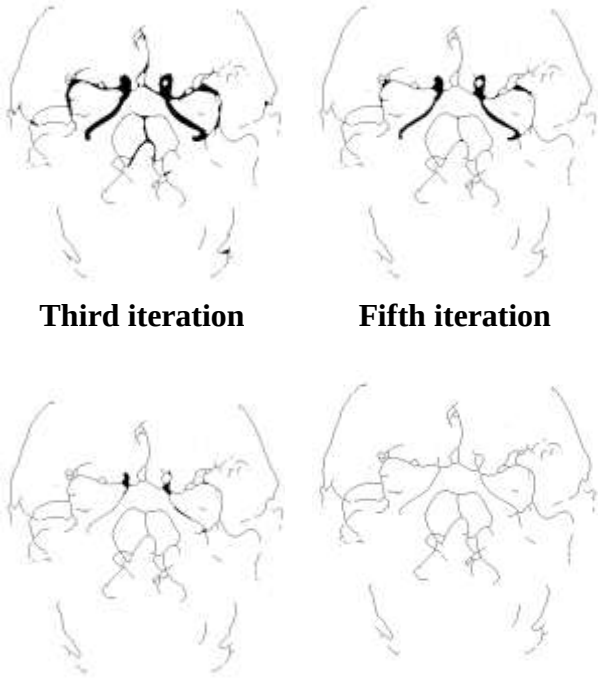

Third iteration **Fifth iteration**

Eighth iteration **After n iterations : Skeleton**

Fig.3 (b). Resulting skeleton after applying an iterative topological thinning on the segmented image

3 BIFURCATION STRUCTURES EXTRACTION:

It is natural to explore and establishes a vascularization relation between two angiographic images because the vascular vessels are robust and stable geometric transformations and intensity change. In this work we use the bifurcation structure, shown on figure 4, for the angiographic images registration.

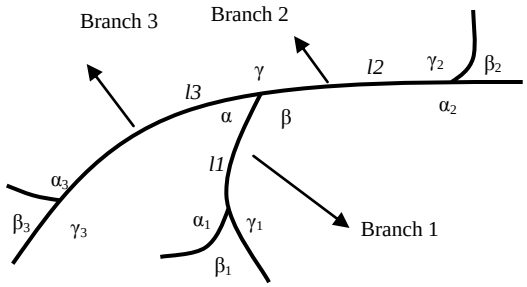

Fig. 4. The bifurcation structure is composed of a master bifurcation point and its three connected neighbors.

The structure is composed of a master bifurcation point and its three connected neighbors. The master point has three branches with lengths numbered 1, 2, 3 and angles numbered α, β, and γ, where each branch is connected to a bifurcation point. The characteristic vector of each bifurcation structure is:

$$\tilde{x} = [l_1, \alpha, \alpha_1, \beta_1, \gamma_1, l_2, \beta, \alpha_2, \beta_2, \gamma_2, l_3, \alpha_3, \beta_3, \gamma_3] \quad (6)$$

Where l_i and α_i are respectively the length and the angle normalized with:

$$\begin{cases} l_i = length \quad of \quad the \quad branch \quad i \Big/ (\sum_{i=1}^{3} lengthes \quad i) \\ \alpha_i = angle \quad of \quad the \quad branch \quad i \quad in \quad \deg rees / 360° \end{cases} \quad (7)$$

To extract the feature vectors of bifurcation structures, several steps must be applied to the reference image and the image to register. We first identify all bifurcation points, isolating those with three connected neighbors before calculating the angles and distances of the structure.

In the angiographic images, bifurcations points are obvious visual characteristics and can be recognized by their T shape with three branches around as indicated in figure 5. Actually, in one image we can find bifurcation points, trifurcation points and end points as shown in figure 5. The last two are characterized respectively by 1 and 4 neighbors. A false bifurcation point, moreover, is too close to another bifurcation point or with a short branch.

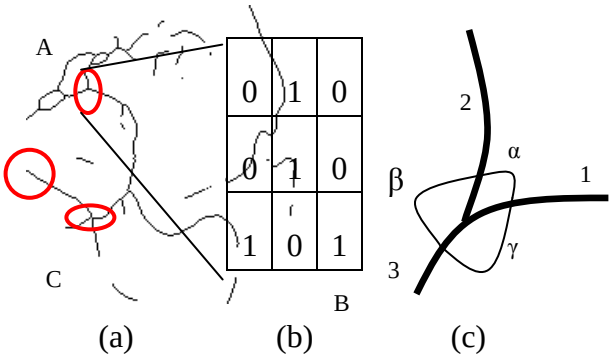

Fig. 5. Features characteristics of an angiographic image (a) Different characteristic points of an angiographic image. A- Bifurcation point. B –End point. C – Trifurcation point. (b) Neighborhood of a bifurcation point. (c) Branching angles of a bifurcation point.

Let P be a point of the image. In a 3x3 window, P has 8 neighbors Vi (i∈{1..8}) which take 1 or 0 as value. Pix is the number of pixel corresponding to 1 in the neighborhood of P is:

$$Pix(P) = \sum_{i=1}^{8} Vi \quad . \quad (8)$$

Finally, the bifurcation points of the image are defined by:

$$PTS\_BIFURCATION = \{THE\ POINTS\ P_{(I,J)}\ AS\ PIX(P_{(I,J)}) \geq 3; (I,J) \in (M,N)\ WHERE\ M\ AND\ N\ ARE\ THE\ DIMENSIONS\ OF\ THE\ IMAGE\} . \quad (9)$$

To calculate the branching angles, we consider a circle of radius R and centered in P [18]. This circle intercepts

the three branches in three points (I1, I2, I3) with coordinates respectively (x_1, y_1), (x_2, y_2) and (x_3, y_3). The angle of each branch relative to the horizontal is given by:

$$\theta_i = arctg(\frac{y_i - y_0}{x_i - x_0}) \quad . \qquad (10)$$

Where θ_i is the angle of the i^{th} branch relative to the horizontal and (x_0, y_0) are the coordinates of the point P. The angel vector of the bifurcation point is written:

$$Angle\_Vector = [\alpha = \theta_2 - \theta_1 \quad \beta = \theta_3 - \theta_2 \quad \gamma = \theta_1 - \theta_3] \qquad (11)$$

Where θ_1, θ_2 et θ_3 correspond to the angles of each branch of the bifurcation point relative to the horizontal. A second steps consists on selecting the best bifurcation points, means those with only three angles. We proceed as shown on algorithm 1. An example is shown in figure 6.

Algorithm 1: Selection of the best bifurcation points

Aim: Extraction of the angles vectors and keeping only those with three angles
Initialization Pbs empty
For each bifurcation point
Calculate the angles vector;
[l, c] ← Size of the angles vector;
If c=3 Pbs ← [Pbs, bifurcation point];
End if
End for

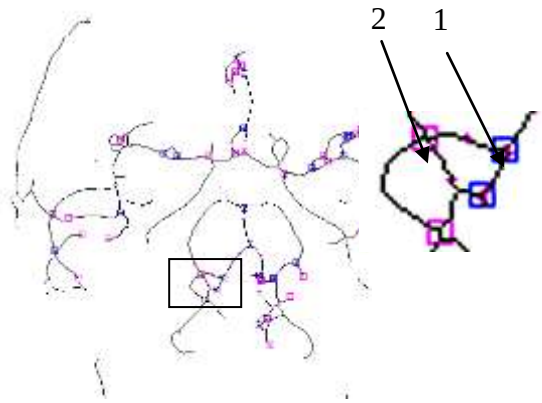

Fig. 6. Tracking of the bifurcation points. 1- Bifurcation point (three neighbors) Angles_vector = [135 90 135]. 2- Trifurcation point (four neighbors).

After the localization of the bifurcation points, we start the tracking of the bifurcation structure. The aim is the extraction of the characteristic vector. To proceed with the tracking, we explore the neighborhood of each bifurcation point. We follow the pixels equal to 1 in this neighborhood until we find a bifurcation point. Let P be the master bifurcation point, P_1, P_2 and P_3 three bifurcation points, neighbors of P. In determining whether there is a connection between P and his entourage, we follow the pixels equal to 1 in its vicinity. This involves taking each time the pixel apart and look in his neighborhood if objects exist and to identify as and when these objects are bifurcation points. We proceed like presented in algorithm 1 and shown in figure 7.

Algorithm 2: Search of the connected neighbors

V ← P
Repeat
In a 3x3 window of V search for Vi = 1

If true then is Vi a bifurcation point
Until Vi corresponds to a bifurcation point.

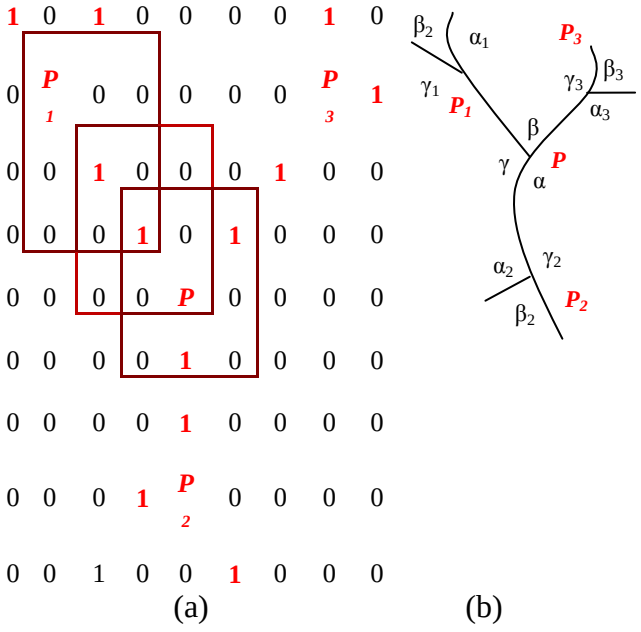

Fig. 7. Feature vector extraction. (a) Example of search in the neighborhood of the master bifurcation point. (b) Master bifurcation point, its neighbors ad its angles and their corresponding angles.

Each point of the structure is defined by its coordinates. So, let (x_0, y_0), (x_1, y_1), (x_2, y_2) et (x_3, y_3) be the coordinates respectively of P, P_1, P_2 et P_3. We have:

$$\begin{cases} l_1 = d(P,P_1) = \sqrt{(x_1 - x_0)^2 + (y_1 - y_0)^2} \\ l_2 = d(P,P_2) = \sqrt{(x_2 - x_0)^2 + (y_2 - y_0)^2} \\ l_3 = d(P,P_3) = \sqrt{(x_3 - x_0)^2 + (y_3 - y_0)^2} \end{cases} \quad (12)$$

$$\begin{cases} \alpha = \theta_2 - \theta_1 = arctg(\frac{x_2 - x_0}{y_2 - y_0}) - arctg(\frac{x_1 - x_0}{y_1 - y_0}) \\ \beta = \theta_3 - \theta_2 = arctg(\frac{x_3 - x_0}{y_3 - y_0}) - arctg(\frac{x_2 - x_0}{y_2 - y_0}) \\ \gamma = \theta_1 \_ \theta_3 = arctg(\frac{x_1 - x_0}{y_1 - y_0}) - arctg(\frac{x_3 - x_0}{y_3 - y_0}) \end{cases} \quad (13)$$

Where l_1, l_2 et l_3 are respectively the branches' lengths that connect P to P_1, P_2 and P_3. θ_1, θ_2 and θ_3 are the angles of the branches relative to the horizontal and α, β and γ are the angles between the branches. Angles and distances have to be normalized according to (7). An example of the characteristic vector of a bifurcation structure is shown in figure 8.

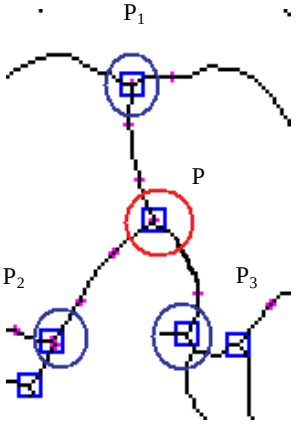

Fig. 8. Characteristic vector for this bifurcation structure is : [37.4833, 173.0218, 105.4992, 149.7120, 104.7886, 43.2781, 130.4748, 110.7722, 80.8111, 168.4165, 32.2800, 56.5033, 195.2551, 70.0168, 94.7279] → Normalization → [0.3315, 0.4806, 0.2930, 0.4158, 0.2910, 0.3828, 0.3624, 0.3077, 0.2244, 0.4678, 0.2855, 0.1569, 0.5423, 0.1944, 0.2631]

4 FEATURE MATCHING :

The matching process seeks for a good similarity criterion among all the pairs of

structures. Let X and Y be the features groups of two images containing respectively a number M_1 and M_2 of bifurcation structures. The similarity measure $s_{i,j}$ on each pair of bifurcation structures is :

$$s_{i,j} = d(x_i, y_j) \quad . \qquad (14)$$

Where x_i and y_j are the characteristic vectors of the i^{th} and the j^{th} bifurcation structures in both images. The term d(.) is the measure of the distance between the characteristic vectors. The considered distance here is the mean of the absolute value of the difference between the feature vectors. We calculate the distance between the characteristic vector of the reference image and all the characteristic vectors of the image to register and we only keep the minimum distance which means two similar bifurcation structures and good candidates for the matching process. Figure 9 illustrates an example of matching process between two bifurcation structures.

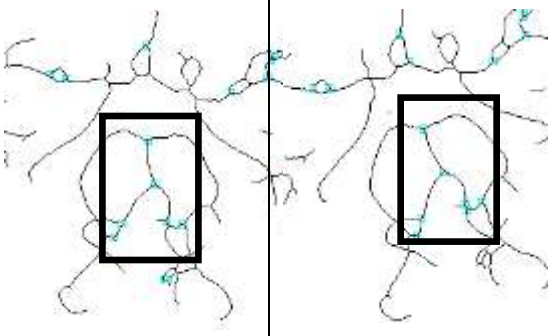

(a)

Characteristic vector 1: [0.3315, 0.4806, 0.2930, 0.4158, 0.2910, 0.3828, 0.3624, 0.3077, 0.2244, 0.4678, 0.2855, 0.1569, 0.5423, 0.1944, 0.2631]

(b)

Characteristic vector 2 : [0.3434, 0.4825, 0.2623, 0.4176, 0.3199, 0.3749, 0.3542, 0.3055, 0.2355, 0.4589, 0.2816, 0.1632, 0.5286, 0.2069, 0.2644]

$s = 0.0101$

Fig. 9. Bifurcation structures matching. (a) Structure of the reference image. (b) Structure of the image to register, result of the 15° rotation of the reference image. The distance between vector 1 and vector 2 is minimum compared with the rest of the characteristic vectors of the image to register. These two structures consist then good candidates for the matching process.

Unlike the three angles of the unique bifurcation point, the characteristic vector of the proposed bifurcation structure contains classified elements, the length and the angle. This structure facilitates the matching process by reducing the multiple correspondences' occurrence as shown on figure 10.

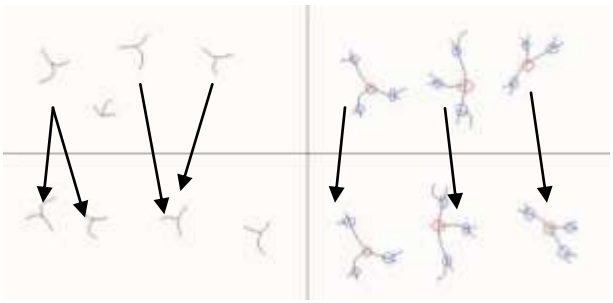

Fig. 10. Matching process. (a) The bifurcation points matching may induce errors due to multiple correspondences. (b) Bifurcation structures matching.

5 REGISTRATION: TRASFORMATION MODEL AND OPTIMIZATION:

Registration is the application of a geometric transformation based on the bifurcation structures on the image to register. We used the linear, affine and projective transformations. We observed that in some cases, the linear transformation provides a better result than the affine transformation but we note that in the general case, the affine transformation is robust enough to

provide a good result, in particular when the image go through distortions. Indeed, this transformation is sufficient to match two images of the same scene taken from the same angle of view but with different positions. The affine transformation has generally four parameters, t_x, t_y, θ and s which transform a point with coordinates (x_1, y_1) into a point with coordinates (x_2, y_2) as follow:

$$\begin{pmatrix} x_2 \\ y_2 \end{pmatrix} = \begin{pmatrix} t_x \\ t_y \end{pmatrix} + s \cdot \begin{pmatrix} \cos\theta & -\sin\theta \\ \sin\theta & \cos\theta \end{pmatrix} \cdot \begin{pmatrix} x_1 \\ y_1 \end{pmatrix} \quad . \tag{15}$$

The 2D affine transformation, in general, may represent the spatial distortions.

$$\begin{pmatrix} x_2 \\ y_2 \end{pmatrix} = \begin{pmatrix} a_{13} \\ a_{23} \end{pmatrix} + \begin{pmatrix} a_{11} & a_{12} \\ a_{21} & a_{22} \end{pmatrix} \cdot \begin{pmatrix} x_1 \\ y_1 \end{pmatrix} \tag{16}$$

The purpose is to apply an optimal affine transformation which parameters realize the best registration. The refinement of the registration and the transformation estimation can be simultaneously reached by:

$$e_{(pq,mn)} = d(M(x_p, y_q), M(x_m, y_n)) \tag{17}$$

Here $M(x_p, y_q)$ and $M(x_m, y_n)$ are respectively the parameters of the estimated transformation from pairs (x_p, y_q) and (x_m, y_n). d(.) is the difference. Of course, successful candidates for the estimation are those with good similarity s. We retain finally the pairs of structures that generate transformation models verifying a minimum error e. e is the mean of the squared difference between models. This guarantees a more efficient registration. Figure 11 shows an example of estimating the parameters of the affine transformation from two structures pairs.

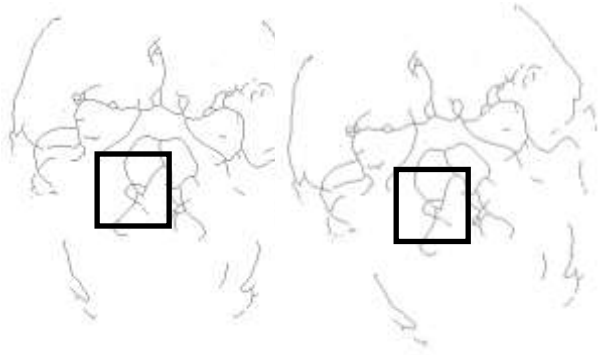

1st pair of structures

Model 1 = [0.9, -0.3, 52.5, 0.2, 1, -102.6, 0, 0, 1]

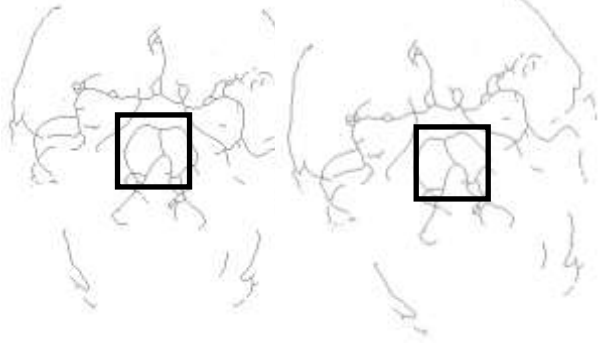

2nd pair of structures

Model 2 = [0.5, 0.4, -23.5, 1.6, -1, 104.6, 0, 0,1]

e = average (Model 2 – Model 1)^2 = 0.0054

(a)

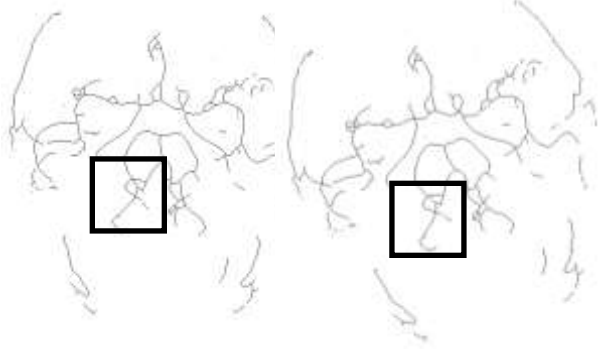

3rd pair of structures

Model 3 = [0.9, -0.3, 52.5 0.2 1, -102.6, 0, 0, 1]

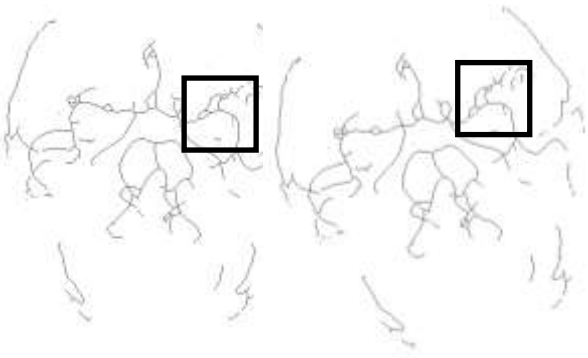

4th pair of structures

Model 4 = [-0.3, 0.7, 293.2, 0.5, 0, -21.5, 0, 0,1]

e= average (Model 4 – Model 3)^2 *= 7168.6*

(b)

Fig. 11. Search of an optimal transformation model for the registration. (a) The error e has a low value; structures are then kept for the final registration. (b) The error has an important value; the 4th pair of structures is then rejected and won't be used in the final registration.

6 EXPERIMENTAL RESULTS:

We proceed to the structures matching using equations (6) and (14) to find the initial correspondence. The structures initially matched are used to estimate the transformation model and refines the correspondence. Figures 12(a) and 12(b) shows two angiographic images. 12(b) has been rotated by 15°. For this pair of images, 19 bifurcation structures has been detected and give 17 good matched pairs. The four best matched structures are shown in figures 12(d) and 12(e). The aligned mosaic images are presented in figure 12(c) and 12(f). Figure 13 presents the registration result for another pair of angiographic images.

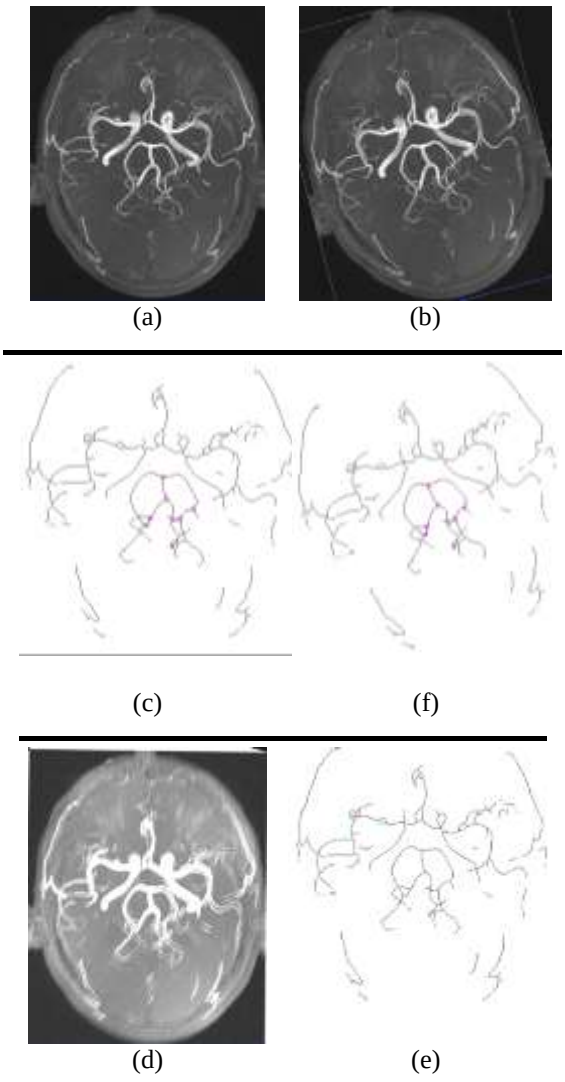

(a) (b) (c) (f) (d) (e)

Fig; 12. Registration result. (a) An angiographic image. (b) A second angiographic image with a 15° rotation compared to the first one. (c)The mosaic angiographic image. (d) Vascular network and matched bifurcation structures of (a). (e) Vascular network and matched bifurcation structures of (b). (f) Mosaic image of the vascular network.

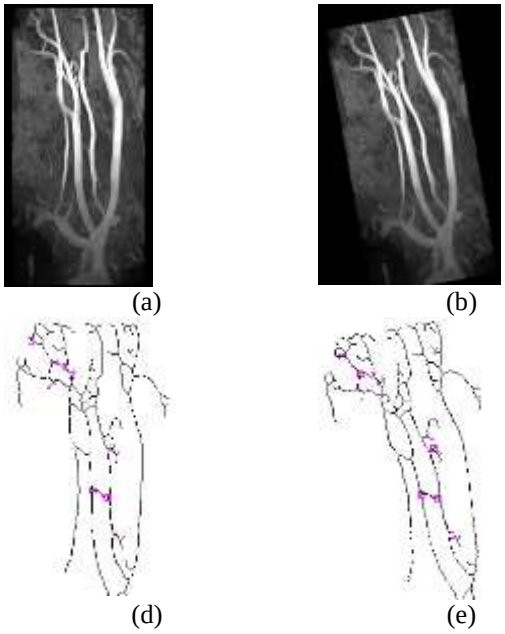

Fig. 13. Registration result for another pair of images. (a) An angiographic image. (b) A second angiographic image with a 15° rotation compared to the first one. (c)The mosaic angiographic image. (d) Vascular network and matched bifurcation structures of (a). (e) Vascular network and matched bifurcation structures of (b). (f) Mosaic image of the vascular network.

We observe that the limitation of the method is that it requires a successful vascular segmentation. Indeed, poor segmentation can infer various artifacts that are not related to the image and thus distort the registration. The advantage of the proposed method is that it works even if the image undergoes rotation, translation and resizing. We applied this method on images which undergoes rotation, translation or re-sizing. The results are illustrated in Figure 14.

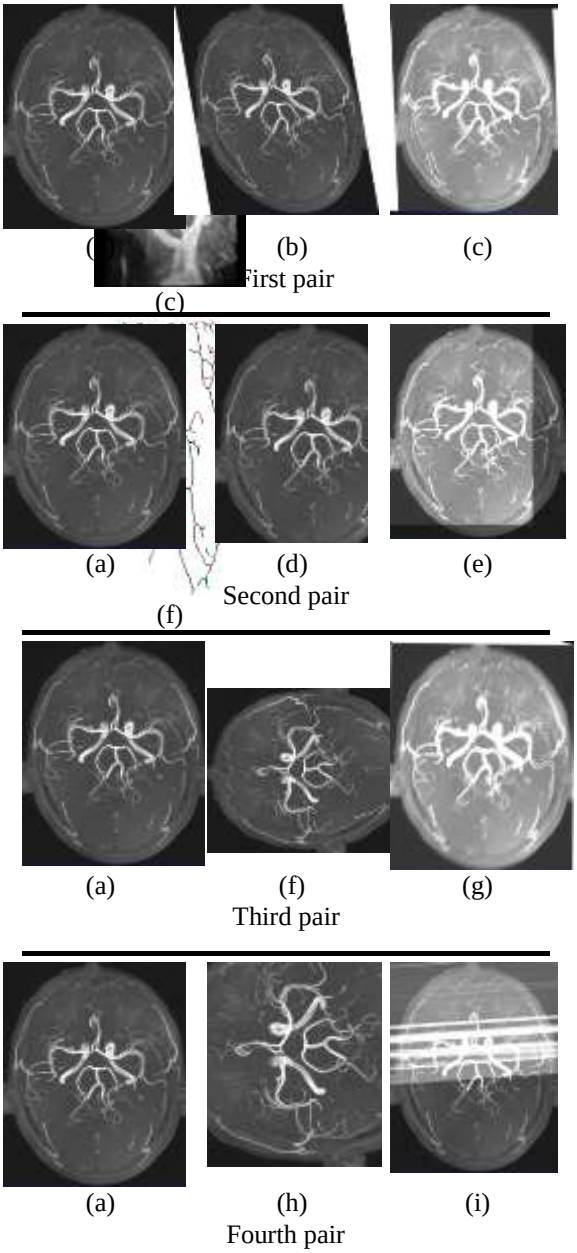

Fig. 14. Registration result on few different pairs of images. (a) Angiographic image. (b) Angiographic image after a 10° declination. (c) Registration result of the first pairs. (d) ARM image after sectioning. (e)Registration result for the second pair. (f) ARM image after 90° rotation. (g) Registration result for the third pair. (h) Angiographic image after 0,8 resizing, sectioning and 90° rotation. (i) Registration result of the fourth pair.

We find that the method works for

images with leans, a sectioning and a rotation of 90 °. For these pairs of images, the bifurcation structures are always 19 in number, with 17 good branching structures matched and finally 4 structures selected to perform the registration. But for the fourth pair of images, the registration does not work. For this pair, we detect 19 and 15 bifurcation structures that yield to 11 matched pairs and finally 4 candidate structures for the registration. We tried to improve the registration by acting on the number of structures to match and by changing the type of transformation. We obtain 2 pairs of candidate structures for the registration of which the result is shown in Figure 15.

(a) (b) (c)

Fig. 15. Registration improvement result. (a) Reference image. (b)Image to register (c) Mosaic image.

7 CONCLUSION:

This paper presents a registration method on the vascular structures in 2D angiographic images. This method involves the extraction of a bifurcation structure consisting of master bifurcation point and its three connected neighbors. Its feature vector is composed of the branches' lengths and branching angles of the bifurcation structure. It is invariant to rotation, translation, scaling and slight distortions. This method is effective when the vascular tree is detected on MRA image.

8 REFERENCES

1. Brown L.G. "A survey of image registration techniques", ACM : Computer surveys, tome 24, n°4, pages 325-376, January 1992.
2. B. Zitova & J. Flusser. "Image registration methods: a survey". Image and Vision Computing, vol. 21, no. 11, pages 977-1000, octobre 2003.
3. Maintz J. B. Antoine & Viergever M. A. "A Survey of Medical Image Registration". Medical Image analysis, volume 2, n°1, pages 1-36, October 1997.
4. Barillot C. Fusion de Données et Imagerie 3D en Médecine, Clearance report, Université de Rennes 1, September 1999.
5. D Hill, P Batchelor, M Holden, D Hawkes, "Medical Image Registration." Phys. Med. Biol.: 46, 2001
6. Passat N. Contribution à la segmentation des réseaux vasculaires cérébraux obtenus en IRM. Intégration de connaissance anatomique pour le guidage d'outils de morphologie mathématique, Thesis report, 28 septembre 2005.
7. S. Ourselin. Recalage d'images médicales par appariement de régions : Application à la création d'atlas histologique 3D. Thesis report, Université Nice-Sophia Antipolis, January 2002.
8. Chillet D, Jomer J, Cool D, Aylward SR. "Vascular Atlas Formation Using a Vessel-to-Image Affine Registration Method", MICCAI 2003, March 2003.
9. Cool D, Chillet D, Kim J, Foskey M, Aylward S, "Tissue-Based Affine Registration of Brain Images to form a Vascular Density Atlas" MICCAI 2003, March 2003.
10. Alexis Roche. Recalage d'images médicales par inférence statistique.

Sciences thesis, Université de Nice Sophia-Antipolis, February 2001.

11. Bondiau P.Y. Mise en œuvre et évaluation d'outils de fusion d'image en radiothérapie. Sciences thesis, Université de Nice-Sophia Antipolis, November 2004.
12. Commowick O. Création et utilisation d'atlas anatomiques numériques pour la radiothérapie. Sciences' Thesis, Université Nice–Sophia Antipolis, February 2007.
13. Styner M, Gerig G, "Evaluation of 2D/3D bias correction with 1+1ES optimization," Technical Report, BIWI-TR-179.
14. Z. Zhang. "Parameter Estimation Techniques: A Tutorial with Application to Conic Fitting". International Journal of Image and Vision Computing, vol. 15, no. 1, pages 59_76, January 1997.
15. Chen L. & X. L. Zhang. "Feature-Based Retinal Image Registration Using Bifurcation Structures", February 2009.
16. Attali. D. Squelettes et graphes de Voronoï 2D et 3D. Doctoral thesis, Université Joseph Fourier - Grenoble I, October 1995.
17. Jlassi H. & Hamrouni K. "Detection of blood vessels in retinal images". International Journal of Image and Graphics, vol. 10, no. 1, pages 57–72, 2010.
18. Jlassi H. & Hamrouni K. « Caractérisation de la rétine en vue de l'élaboration d'une méthode biométrique d'identification de personnes », SETIT 2005, March 2005.